

## Single, double, and triple Auger decay probabilities of $C^+(1s2s^22p^2^2D, ^2P)$ resonances

Fuyang Zhou, Yulong Ma, and Yizhi Qu\*

College of Material Sciences and Optoelectronic Technology, University of Chinese Academy of Sciences, Beijing 100049, China

(Received 14 April 2016; published 3 June 2016)

Single, double, and triple Auger decay rates of  $C^+(1s2s^22p^2^2D, ^2P)$  resonances were calculated in the framework of perturbation theory. The direct double Auger decay probabilities were calculated by using the approximate formulas according to the knockout and shakeoff mechanisms, in which the knockout mechanism was found to be dominant. Then the knockout mechanism was employed to investigate the complex triple Auger decay process, and the calculated rates have good agreement with the available experimental values.

DOI: 10.1103/PhysRevA.93.060501

For light elements, the Auger process is the dominant decay channel of hole states. Investigations of Auger decay are of great interest to various application fields such as plasma physics [1,2], astrophysics [3,4], and x-ray laser schemes [5,6]. In the normal Auger process, it emits one of the outer-shell electrons in the transition of filling a vacancy by another outer-shell electron. If the vacancy is in a deep inner shell, the direct double Auger processes are reached when two outer-shell electrons are ejected simultaneously in the filling of a vacancy. Meanwhile, if the single Auger decay produces an autoionizing state decayed via another Auger transition, this process in which two electrons are emitted sequentially is called cascade double Auger decay. Since the first observation of the double Auger decay in 1965 [7], many accurate experiments have been done, in particular the measurements of the ratio of double to single Auger decay rates [8–11]. Meanwhile, accurate *ab initio* methods have been developed to calculate the direct double Auger decay probability [12–15]. Due to the complexity of the three-electron interaction involved, the approximate formulas according to knockout and shakeoff mechanisms are generally employed [14–17].

Recently, the first direct triple Auger decay process with simultaneous emission of three electrons has been observed by measuring single, double, and triple ionization of  $C^+(1s2s^22p^2^2D, ^2P)$  resonances [18]. The experiment quantified the probabilities of direct triple Auger decay which is the only possible mechanism producing  $C^{4+}(1s^2)$  via  $C^+(1s2s^22p^2^2D, ^2P)$  resonances [18]. However, no theoretical prediction for direct triple Auger decay is available due to the complexity of the four-body process. In this paper, we calculated the direct triple Auger rates of  $C^+(1s2s^22p^2^2D, ^2P)$  based on the knockout mechanism, in which the multiple Auger decay process was decomposed into a sequence of two-electron processes.

In the first-order perturbation theory, the single Auger decay rate can be expressed as [19,20]

$$A_{\alpha\beta}^1 = \left| \langle \psi_{\beta}^+ | \sum_{i<j}^N \frac{1}{r_{ij}} | \psi_{\alpha} \rangle \right|^2, \quad (1)$$

where  $\psi_{\alpha}$  is the initial autoionizing state with  $N$  electrons and  $\psi_{\beta}^+$  is the final state of the system which has  $N-1$  electrons

plus a continuum electron,

$$|\psi_{\beta}^+\rangle = |\psi_{\beta,\kappa}; J_T M_T\rangle. \quad (2)$$

Here  $\kappa$  is the relativistic angular quantum number of the free electron,  $J_T$  and  $M_T$  are the total angular momentum and magnetic quantum number, respectively.

In the independent-particle model, the matrix element  $\langle \psi_{\gamma}^{2+} | \sum_{i<j}^N \frac{1}{r_{ij}} | \psi_{\alpha} \rangle$  of the direct double Auger decay is zero since the initial and the final wave functions differ by more than two single-electron orbitals. In this case, the many-electron correlations should be taken into account. In order to simplify the computation of direct double Auger rate, we employed the approximate formulas according to the knockout (KO) and shakeoff (SO) mechanisms, which were generally invoked for a simultaneous two-electron emission process [14,15].

In the KO mechanism, the direct double Auger process is decomposed into a primary single Auger decay and a subsequent electron-electron inelastic scattering process, which can be calculated separately. The direct double Auger rate can be expressed as

$$A_{\text{KO}}^2 = \sum_{\beta} A_{\alpha\beta}^1 \Omega_{\beta\gamma}(\varepsilon_0), \quad (3)$$

where  $A_{\alpha\beta}^1$  is the single Auger rate from the initial autoionizing state  $\psi_{\alpha}$  to middle state  $\psi_{\beta}^+$ , and  $\Omega_{\beta\gamma}(\varepsilon_0)$  is the collision strength of the inelastic scattering of the “intermediate” Auger electron upon the middle state  $\psi_{\beta}^+$ .  $\varepsilon_0$  is the free-electron energy in the first single Auger decay process, which satisfies the energy conservation law. The KO mechanism can be considered as the simple picture [14,21]: The ejection of the second electron should resemble electron-impact ionization by the continuum electron produced by the first single Auger decay process.

The direct double Auger rate in the SO mechanism can be defined as

$$A_{\text{SO}}^2 = \sum_{\beta} A_{\alpha\beta}^1 |\langle \psi_{\gamma}^{2+} | \psi_{\beta}^+ \rangle|^2, \quad (4)$$

where the matrix element  $\langle \psi_{\gamma}^{2+} | \psi_{\beta}^+ \rangle$  is the overlap integral between the two wave functions of the middle and final states with two Auger electrons being emitted. The calculation of the overlap integral is straightforward with one less continuum electron in both wave functions [17]. In this purely quantum mechanism, the first Auger electron is ejected rapidly and the ejection of the second Auger electron is due to relaxation

\*yzqu@ucas.ac.cn

TABLE I. Single Auger decay probability  $A^1$  ( $s^{-1}$ ) for the main channels of  $C^+$   $1s$  hole states.

Initial state	Final state	RATIP		FAC	
		$\Delta E$ (eV)	$A^1$	$\Delta E$ (eV)	$A^1$
$1s2s^22p^2^2P_{1/2}$	$1s^22s2p^1P_1$	249.302	$2.160 \times 10^{13}$	250.538	$2.736 \times 10^{13}$
	$1s^22p^2^3P_0$	245.719	$2.029 \times 10^{13}$	246.269	$2.124 \times 10^{13}$
	$1s^22p^2^3P_1$	245.717	$4.149 \times 10^{13}$	246.268	$4.300 \times 10^{13}$
	$1s^22p^2^3P_2$	245.714	$2.467 \times 10^{12}$	246.266	$1.894 \times 10^{12}$
	Total rate		$8.655 \times 10^{13}$		$9.668 \times 10^{13}$
$1s2s^22p^2^2P_{3/2}$	$1s^22s2p^1P_1$	249.315	$2.161 \times 10^{13}$	249.905	$2.725 \times 10^{13}$
	$1s^22p^2^3P_0$	245.732	$4.900 \times 10^{11}$	245.636	$3.829 \times 10^{11}$
	$1s^22p^2^3P_1$	245.729	$1.128 \times 10^{13}$	245.634	$1.152 \times 10^{13}$
	$1s^22p^2^3P_2$	245.726	$5.244 \times 10^{13}$	245.633	$5.424 \times 10^{13}$
	Total rate		$8.670 \times 10^{13}$		$9.660 \times 10^{13}$
$1s2s^22p^2^2D_{3/2}$	$1s^22s^2^1S_0$	263.275	$5.095 \times 10^{13}$	264.103	$5.500 \times 10^{13}$
	$1s^22s2p^3P_1$	256.473	$1.138 \times 10^{13}$	256.995	$1.104 \times 10^{13}$
	$1s^22s2p^1P_1$	249.073	$3.563 \times 10^{13}$	249.905	$4.250 \times 10^{13}$
	$1s^22p^2^1D_2$	243.385	$6.559 \times 10^{13}$	243.887	$6.234 \times 10^{13}$
	Total rate		$1.740 \times 10^{14}$		$1.839 \times 10^{14}$
$1s2s^22p^2^2D_{5/2}$	$1s^22s^2^1S_0$	263.265	$5.107 \times 10^{13}$	264.093	$5.498 \times 10^{13}$
	$1s^22s2p^3P_2$	256.459	$1.677 \times 10^{13}$	256.982	$1.590 \times 10^{13}$
	$1s^22s2p^1P_1$	249.064	$3.548 \times 10^{13}$	249.895	$4.237 \times 10^{13}$
	$1s^22p^2^1D_2$	243.375	$6.528 \times 10^{13}$	243.877	$6.235 \times 10^{13}$
	Total rate		$1.739 \times 10^{14}$		$1.838 \times 10^{14}$

following the sudden change of the atomic potential. In the high-energy limit for the Auger electron, this sudden approximation can properly describe the direct double Auger decay process.

In the knockout and shakeoff mechanisms, the direct double Auger process is decomposed into a primary single Auger decay and a subsequent two-electron process, which can be calculated separately. The single Auger rates were obtained in the framework of distorted wave approximation implemented by the RATIP package [20], which is based on the multiconfiguration Dirac-Fock (MCDF) method [22,23]. But the present RATIP package is restricted to atomic processes with just one electron within the continuum [20], and it cannot be used to compute the collision strengths and overlap integrals. Therefore, the collision strengths and overlap integrals are computed by employing Flexible Atomic Code (FAC) [19], which also uses the DW approximation for continuum

processes. In FAC, the formula for collisional ionization is obtained based on the factorization-interpolation method developed for the calculation of electron-impact excitation cross sections [24] by replacing one bound orbital in the final state with the free orbital of the ejected electron. In this work, we extended FAC to calculate the collision strengths and overlap integrals of the subsequent process after primary single Auger decay, in which the angular momenta of the first Auger electron and complete system are fixed. Meanwhile, we also used the FAC package for the computation of single Auger decay.

On the other hand, the single Auger decay might also produce an autoionizing state, which can decay through a second Auger transition; the rate of this cascade double Auger decay can be simply obtained from the product of the first single Auger rate and branching ratio for the autoionizing state decay into the final state  $|\psi_\gamma^{2+}\rangle$ .

TABLE II. Energies  $E$  (eV) and lifetime widths  $\Gamma$  (meV) of the  $C^+(1s2s^22p^2^2D, ^2P)$  resonances.

State	$E$ (eV) <sup>a</sup>	$E$ (eV) <sup>b</sup>	$E$ (eV) <sup>c</sup>	$E$ (eV) <sup>d</sup>	$E$ (eV) <sup>e</sup>
$1s2s^22p^2^2P$	288.11	286.96	288.63	$288.40 \pm 0.03$	$288.59 \pm 0.2$
$1s2s^22p^2^2D$	287.87	286.32	287.96	$287.93 \pm 0.03$	$287.91 \pm 0.2$
State	$\Gamma$ (meV) <sup>a</sup>	$\Gamma$ (meV) <sup>b</sup>	$\Gamma$ (meV) <sup>c</sup>	$\Gamma$ (meV) <sup>f</sup>	$\Gamma$ (meV) <sup>d</sup>
$1s2s^22p^2^2P$	57	64	56	62	$59 \pm 6$
$1s2s^22p^2^2D$	114	121	102	103	$105 \pm 15$

<sup>a</sup>RATIP, present work.<sup>b</sup>FAC, present work.<sup>c</sup> $R$  matrix [25].<sup>d</sup>Advanced light source, experimental work [25].<sup>e</sup>Dual-plasma, experimental work [27].<sup>f</sup> $R$  matrix [26].

TABLE III. Double Auger decay rates  $A^2(s^{-1})$  for the main channels of  $C^+(1s2s^22p^2{}^2D, {}^2P)$  resonances.

Initial state	Final state	$A_{KO}^2$	$A_{SO}^2$
$1s2s^22p^2{}^2P_{1/2}$	$1s^22s\ 1S_0$	$4.459 \times 10^{11}$	$1.516 \times 10^{10}$
	$1s^22p\ 2P_{1/2}$	$9.458 \times 10^{11}$	$6.464 \times 10^{10}$
	$1s^22p\ 2P_{3/2}$	$9.630 \times 10^{11}$	$6.672 \times 10^{10}$
	Total	$2.420 \times 10^{12}$	$1.523 \times 10^{11}$
$1s2s^22p^2{}^2P_{3/2}$	$1s^22s\ 1S_0$	$3.853 \times 10^{11}$	$1.535 \times 10^{10}$
	$1s^22p\ 2P_{1/2}$	$4.665 \times 10^{11}$	$3.349 \times 10^{10}$
	$1s^22p\ 2P_{3/2}$	$1.398 \times 10^{12}$	$9.807 \times 10^{10}$
	Total	$2.311 \times 10^{12}$	$1.527 \times 10^{11}$
$1s2s^22p^2{}^2D_{3/2}$	$1s^22s\ 1S_0$	$2.181 \times 10^{12}$	$2.015 \times 10^{11}$
	$1s^22p\ 2P_{1/2}$	$9.871 \times 10^{11}$	$7.111 \times 10^{10}$
	$1s^22p\ 2P_{3/2}$	$1.416 \times 10^{12}$	$1.099 \times 10^{11}$
	Total	$4.701 \times 10^{12}$	$3.986 \times 10^{11}$
$1s2s^22p^2{}^2D_{5/2}$	$1s^22s\ 1S_0$	$2.522 \times 10^{12}$	$2.022 \times 10^{11}$
	$1s^22p\ 2P_{1/2}$	$5.551 \times 10^{11}$	$5.263 \times 10^{10}$
	$1s^22p\ 2P_{3/2}$	$1.517 \times 10^{12}$	$1.285 \times 10^{11}$
	Total	$4.711 \times 10^{12}$	$3.993 \times 10^{11}$

Since the single Auger process is the first step of the KO and SO mechanisms, the accurate single Auger rate is pivotal in the subsequent calculation of multiple Auger rate. In this work, the single Auger rates were calculated by using RATIP and FAC codes. Both the RATIP and FAC codes are based on standard Racah algebra techniques, which assumes that the orbital sets for the initial- and final-state wave functions are the same. But in the triple Auger decay process, four ionized states from  $C^+$  to  $C^{4+}$  are involved. In the KO and SO mechanisms, the wave functions of only two successive ions are connected; thus we optimize the orbitals of two successive ions separately. For example, the wave functions of the orbitals in calculation of single Auger decay are optimized to accommodate the contributions from the ground configurations of  $C^+$  and  $C^{2+}$  ions, and these in the calculation of collision strengths and overlap integrals for direct double Auger decay are optimized to accommodate the contributions from the ground configurations of  $C^{2+}$  and  $C^{3+}$  ions. Furthermore, the configuration interaction (CI) approach was carried out to take the electron correlation effects into account. For each ionic stage, the configurations obtained by single and double excitations from the respective ground configurations to active sets of  $n \leq 4$  were considered.

TABLE IV. Ratios of triple to double to single Auger decay rates of  $C^+(1s2s^22p^2{}^2D, {}^2P)$  resonances. The total double Auger rates are the sum of cascade and direct double Auger rates.

Initial states	Double Auger (DA) decay			Expt. [18] Total DA	Triple Auger decay	
	Cascade DA	This work			This work	Expt. [18]
		Direct DA	Total DA			
$1s2s^22p^2{}^2P$	0.132%	2.730% <sup>a</sup> 2.907% <sup>b</sup>	2.862% <sup>a</sup> 3.039% <sup>b</sup>	3.22%	0.0177%	0.0129%
$1s2s^22p^2{}^2D$	0.045%	2.705% <sup>a</sup> 2.934% <sup>b</sup>	2.750% <sup>a</sup> 2.979% <sup>b</sup>	2.59%	0.0174%	0.0128%

<sup>a</sup>Including contribution from only KO mechanism.

<sup>b</sup>Including contribution from both KO and SO mechanisms.

Table I presents the single Auger decay probabilities  $A^1(s^{-1})$  for the main channels of  $C^+1s$  hole states. General agreement is found between the results from the RATIP and FAC codes. The most important pathways originate from the configurations of  $1s^22s^2$ ,  $1s^22s2p$ , and  $1s^22p^2$ , which contribute most of the total rate. In our calculations, the decay channels that originated from the levels which are higher than the ionization potential of  $C^{2+}$  contribute only about 0.1% of total rates. This result reveals the contribution of a weak cascade double Auger decay process.

The accuracy of the total single Auger rates can be examined by comparing the lifetime widths with the experimental values. The nature linewidths of the  $C^+$  ions  $1s2s^22p^2{}^2P, {}^2D$  terms were experimentally determined by Schlachter *et al.* from photoexcitation spectra [25]. In Table II our calculated average lifetime widths of the  $1s2s^22p^2{}^2P, {}^2D$  terms are compared with the experimental values, as well as the  $R$ -matrix calculations by McLaughlin *et al.* [26] and Schlachter *et al.* [25]. General agreement is found among theoretical and experimental lifetime widths. All the theoretical predictions of lifetime widths are within or very close to the error bars of the experimental lifetime widths. Compared to the experimental value, RATIP code provides better results of both excitation energies and lifetime widths than FAC. As mentioned above, the calculations of primary single Auger decay and a subsequent two-electron process are completely separate in the present work. Therefore, we used the RATIP results of single Auger decay rates to calculate double Auger rates.

After obtaining the single Auger decay rates, the direct double Auger probabilities were calculated using KO and SO mechanisms, which are presented in Table III. The most important double Auger decay channels of  $1s2s^22p^2{}^2P_{1/2, 3/2}$  states are from configuration  $1s^22p$ , and the next strongest channel is from configuration  $1s^22s$ . For the  $1s2s^22p^2{}^2D$  term, the strongest double Auger decay channel originates from configuration  $1s^22s$ . The contributions from ground and low-lying states of  $C^{3+}$  account for most of the total double Auger rate; as a result, the cascade triple Auger decay process is negligible. For all the dominant decay channels, the contribution of the KO mechanism is about an order of magnitude larger than that of the SO mechanism, so KO is the dominant mechanism to describe the direct double Auger process for the  $C^+1s$  hole state.

For the multiple Auger decay process of  $C^+1s2s^22p^2{}^2P, {}^2D$  terms, Müller *et al.* [18] obtained the ratios

of triple to double to single Auger decay rates, which are of the order of  $10^{-4} : 10^{-2} : 1$ , by measuring the fractions of total cross sections for single, double, and triple resonant photoionization. In Table IV our calculated double Auger decay branching ratios are presented and compared with their observed values. The experimental ratios of double to single Auger decay rates of  $1s2s^22p^2^2P, ^2D$  terms are 3.22% and 2.59%, respectively, in which the systematic uncertainty of the measured cross sections for both single and double ionization is  $\pm 15\%$  [18]. The theoretical cascade double Auger decay branching ratios of  $1s2s^22p^2^2P, ^2D$  terms are only 0.132% and 0.045%, respectively, which are even smaller than the uncertainties of total double Auger rates. By considering both cascade and direct mechanisms, our calculated total double Auger decay branching ratios are also presented in Table IV. The total double Auger decay branching ratios of  $1s2s^22p^2^2P, ^2D$  terms are 3.039% and 2.979% when contributions from both KO and SO mechanisms are included, and they are 2.862% and 2.750% when only the KO mechanism is considered. The results are in agreement with the experimental values, and indicate that the KO mechanism is dominant.

Since KO is the dominant mechanism for double Auger decay of a  $C^+ 1s$  hole, one can decompose the three-electron double Auger process into a sequence of two-electron processes within the KO model. Then the triple Auger rate has the form

$$\begin{aligned} A_{\alpha\gamma\delta}^3 &= A_{\alpha\gamma}^2 \int_0^{E_{\max}/2} \rho_{\alpha\gamma}(\varepsilon) [\Omega_{\gamma\delta}(\varepsilon) + \Omega_{\gamma\delta}(E_{\max} - \varepsilon)] d\varepsilon \\ &= A_{\alpha\gamma}^2 \int_0^{E_{\max}} \rho_{\alpha\gamma}(\varepsilon) \Omega_{\gamma\delta}(\varepsilon) d\varepsilon, \end{aligned} \quad (5)$$

where  $A_{\alpha\gamma}^2$  is the double Auger rate from the initial autoionizing state  $\psi_\alpha$  to middle state  $\psi_\gamma^{2+}$  with  $N-2$  bound electrons and two continuum ones.  $\Omega_{\gamma\delta}(\varepsilon)$  and  $\Omega_{\gamma\delta}(E_{\max} - \varepsilon)$  are the collision strength of the inelastic scattering final state  $\psi_\delta^{3+}$  by the two “intermediate” Auger electrons, in which  $E_{\max}$  is the total energy of the continuum electrons in the primary double Auger decay process.  $\rho_{\alpha\gamma}(\varepsilon)$  is the probability of the distribution of the total energy between two continuum electrons, which is dependent on different mechanisms and the state of the first Auger electron. Since KO is the dominant mechanism, in which the ejection of the second electron is due to the inelastic scattering of the “intermediate” Auger electron, the  $\rho_{\alpha\gamma}(\varepsilon)$  in our calculations was approximately obtained by using a single energy differential cross section in the binary-encounter model [28]. In Fig. 1, we illustrate the energy distribution of the Auger electrons for double Auger decay  $1s2s^22p^2^2P \rightarrow 1s^22p^2P$ , which are calculated by using the binary-encounter model and the simpler Mott model [28,29]. The U-shaped energy distribution in double Auger decay

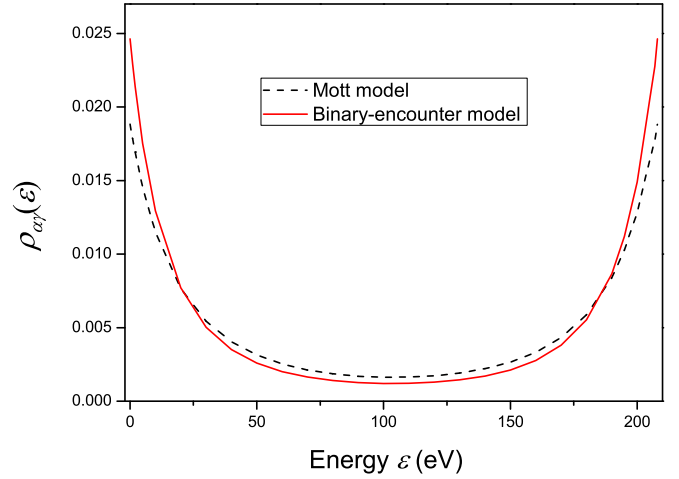


FIG. 1. Energy distribution of the Auger electrons for double Auger decay  $1s2s^22p^2^2P \rightarrow 1s^22p^2P$ .

shows a preference for asymmetric energy sharing consisting of a slow Auger electron and a fast one, which is similar to the case for Ne  $K$ -LLL double Auger decay [14,30]. According to our separate test calculations of the energy distribution for Ne  $K$ -LLL double Auger decay, the binary-encounter model results agree well with the experimental values [30], and has better agreement than the Mott model. The difference in final triple Auger rates between the binary-encounter and Mott models is about 10%, which is relatively small compared with experimental and theoretical overall uncertainty.

For triple Auger decay of the  $C^+ 1s$  hole state, the only possible final state is  $C^{4+}(1s^2)$ . In Table IV, the calculated triple Auger decay branching ratios for  $1s2s^22p^2^2P, ^2D$  terms are 0.0177% and 0.0174%, respectively, compared with the experimental values 0.0129% and 0.0128%. The agreement is relatively good considering that the estimate of the systematic uncertainty of the measured triple ionization cross sections is 50% in the experiment [18]. Using the KO mechanism this approach provides an approximate quantitative prediction of triple Auger decay rates of  $C^+$ .

In conclusion, the knockout mechanism was successfully applied to the calculations of the double and triple Auger decay rates for the  $C^+ 1s$  hole state. The theoretical results of the total triple Auger decay probabilities are in good agreement with the recent experimental values. More accurate theoretical and experimental results of triple Auger rates for other systems are expected for examining the validity of the knockout model.

This work was supported by the NSAF (Grant No. U1330117). We are grateful to Dr. Jiguang Li and Prof. Jiaolong Zeng for their helpful discussions about the calculations of single and double Auger rates.

- [1] B. Denne, E. Hinnov, J. Ramette, and B. Saoutic, *Phys. Rev. A* **40**, 1488 (1989).  
 [2] J. Y. Dai, Y. Hou, and J. M. Yuan, *Phys. Rev. Lett.* **104**, 245001 (2010).

- [3] V. Jonauskas, P. Bogdanovich, F. P. Keenan, R. Kisielius, M. E. Foord, R. F. Heeter, S. J. Rose, G. J. Ferland, and P. H. Norrington, *Astron. Astrophys.* **455**, 1157 (2006).  
 [4] T. R. Kallman and P. Palmeri, *Rev. Mod. Phys.* **79**, 79 (2007).

- [5] A. Lapierre and E. J. Knystautas, *J. Phys. B: At., Mol. Opt. Phys.* **33**, 2245 (2000).
- [6] B. Lin, H. G. Berry, T. Shibata, A. E. Livingston, H.-P. Garnir, T. Bastin, J. Déséquelles, and I. Savukov, *Phys. Rev. A* **67**, 062507 (2003).
- [7] T. A. Carlson and M. O. Krause, *Phys. Rev. Lett.* **14**, 390 (1965).
- [8] S. Brünken, Ch. Gerth, B. Kanngießer, T. Luhmann, M. Richter, and P. Zimmermann, *Phys. Rev. A* **65**, 042708 (2002).
- [9] Y. Tamenori, K. Okada, S. Tanimoto, T. Ibuki, S. Nagaoka, A. Fujii, Y. Haga, and I. H. Suzuki, *J. Phys. B: At., Mol. Opt. Phys.* **37**, 117 (2004).
- [10] J. Viefhaus, S. Cvejanović, B. Langer, T. Lischke, G. Prümper, D. Rolles, A. V. Golovin, A. N. Grum-Grzhimailo, N. M. Kabachnik, and U. Becker, *Phys. Rev. Lett.* **92**, 083001 (2004).
- [11] M. Nakano, Y. Hikosaka, P. Lablanquie, F. Penent, S.-M. Huttula, I. H. Suzuki, K. Soejima, N. Kouchi, and K. Ito, *Phys. Rev. A* **85**, 043405 (2012).
- [12] M. S. Pindzola and D. C. Griffin, *Phys. Rev. A* **36**, 2628 (1987).
- [13] M. S. Pindzola, F. Robicheaux, and J. Colgan, *Phys. Rev. A* **72**, 022709 (2005).
- [14] M. Ya. Amusia, I. S. Lee, and V. A. Kilin, *Phys. Rev. A* **45**, 4576 (1992).
- [15] J. Zeng, P. Liu, W. Xiang, and J. Yuan, *Phys. Rev. A* **87**, 033419 (2013).
- [16] J. A. R. Samson, *Phys. Rev. Lett.* **65**, 2861 (1990).
- [17] J. Zeng, P. Liu, W. Xiang, and J. Yuan, *J. Phys. B: At., Mol. Opt. Phys.* **46**, 215002 (2013).
- [18] A. Müller, A. Borovik, Jr., T. Buhr, J. Hellhund, K. Holste, A. L. D. Kilcoyne, S. Klumpp, M. Martins, S. Ricz, J. Viefhaus, and S. Schippers, *Phys. Rev. Lett.* **114**, 013002 (2015).
- [19] M. F. Gu, *Can. J. Phys.* **86**, 675 (2008).
- [20] S. Fritzsche, *Comput. Phys. Commun.* **183**, 1525 (2012).
- [21] T. Pattard and J. Burgdörfer, *Phys. Rev. A* **63**, 020701 (2001).
- [22] I. P. Grant, *Relativistic Quantum Theory of Atoms and Molecules* (Springer, New York, 2007).
- [23] F. A. Parpia, C. Froese Fischer, and I. P. Grant, *Comput. Phys. Commun.* **94**, 249 (1996).
- [24] A. Bar-Shalom, M. Klapisch, and J. Oreg, *Phys. Rev. A* **38**, 1773 (1988).
- [25] A. S. Schlachter, M. M. Sant'Anna, A. M. Covington, A. Aguilar, M. F. Gharaibeh, E. D. Emmons, S. W. J. Scully, R. A. Phaneuf, G. Hinojosa, I. Álvarez, C. Cisneros, A. Müller, and B. M. McLaughlin, *J. Phys. B: At., Mol. Opt. Phys.* **37**, L103 (2004).
- [26] B. M. McLaughlin, J. M. Bizau, D. Cubaynes, M. M. Al. Shorman, S. Guilbaud, I. Sakho, C. Blancard, and M. F. Gharaibeh, *J. Phys. B: At., Mol. Opt. Phys.* **47**, 115201 (2014).
- [27] E. Jannitti, M. Gaye, M. Mazzoni, P. Nicolosi, and P. Villorosi, *Phys. Rev. A* **47**, 4033 (1993).
- [28] Y.-K. Kim and M. E. Rudd, *Phys. Rev. A* **50**, 3954 (1994).
- [29] N. F. Mott, *Proc. R. Soc. London, Ser. A* **126**, 259 (1930).
- [30] J. Viefhaus, A. N. Grum-Grzhimailo, N. M. Kabachnik, and U. Becker, *J. Electron Spectrosc. Relat. Phenom.* **141**, 121 (2004).